THE JOURNAL OF PHYSICAL CHEMISTRY A

Article

pubs.acs.org/JPCA

Modulation of the L_a/L_b Mixing in an Indole Derivative: A Position-Dependent Study Using 4-, 5-, and 6-Fluoroindole

Josefin Wilke,[†,∥] Martin Wilke,[†,∥] Christian Brand,[†,§] J. Dominik Spiegel,[‡] Christel M. Marian,[‡] and Michael Schmitt*[,†]

[†]Institut für Physikalische Chemie I, Heinrich-Heine-Universität, D-40225 Düsseldorf, Germany

[‡]Institut für Theoretische Chemie und Computerchemie, Heinrich-Heine-Universität, D-40225 Düsseldorf, Germany

[§]Faculty of Physics, VCQ, University of Vienna, Boltzmanngasse 5, A-1090 Vienna, Austria

Supporting Information

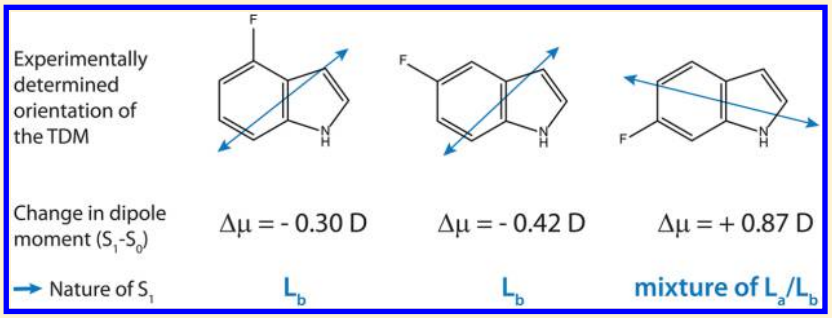

ABSTRACT: The lowest two electronically excited singlet states of indole and its derivatives are labeled as L_a or L_b, based on the orientation of the transition dipole moment (TDM) and the magnitude of the permanent electric dipole moment. Rotationally resolved electronic Stark spectroscopy in combination with high level *ab initio* calculations offers the possibility to determine these characteristics and thus the electronic nature of the excited states. In the present contribution this approach was pursued for the systems 4- and 6-fluoroindole and the results compared to the previously investigated system 5-fluoroindole. Changing the position of the fluorine atom from 5 to 4 or 6 is accompanied by an increasing amount of L_a character in the S_1 state. This dramatically influences the orientation of the TDM and erases its ability to be a reasonable identifier of the nature of the excited states for both molecules. However, for 4-fluoroindole, where the influence of the L_a is weak, the nature of the S_1 state can still be assigned to be mainly L_b based on the excited state dipole moment. For 6-fluoroindole, this is not the case anymore, and the L_a/L_b nomenclature completely breaks down due to heavily mixed excited states.

INTRODUCTION

Non-natural amino acids greatly enhance the spectrum of fluorescent probes in proteins due to their tailor-made photophysical properties.[1−3] Within this group, derivatives of the canonical amino acids have the asset that they keep the perturbation of the protein structure to a minimum.[4−7] However, to make full use of the potential of non-natural amino acids their photophysical properties have to be known. As shown for a number of derivatives of tryptophan[4,6] and its chromophore indole,[8−10] the introduction of substituents may alter the energetic ordering of the two lowest excited singlet states, denoted as ^1L_a and ^1L_b, which are responsible for the emission properties of the molecule. Non-natural amino acids may also be used in order to study solvation processes. Replacing tryptophan by 5-cyanotryptophan allows for a site-specific investigation to probe a protein's hydration,[11] since 5-cyanotryptophan fluorescence quantum yield and consequently its radiative lifetime is considerably different from that of tryptophan.

The L_a/L_b nomenclature was introduced by Platt[12] in order to make a classification of the $\pi\pi^*$ states of cata-condensed hydrocarbons. It is deduced using the model of a free electron traveling in a loop around the perimeter of the molecule. In systems with n rings, the total angular momentum may take the values 0, 1, ..., which are designated A, B, ..., and $2n$, $2n + 1$, ..., for which the designation K, L, ..., was chosen. All states, despite the A state are doubly degenerate. Beside highly symmetric molecules like benzene in which all atoms are situated on a perimeter constant potential, this degeneracy is lifted and the two states are distinguished by the subscript a or b. The a-labeled states have their transition dipole moment direction in a way, that it runs through atoms in the perimeter, while the transition dipole of the b states runs through bonds (the wave functions have a nodal plane that cuts through the cross-link bond of the rings (a) or is perpendicular to it (b)). While the transition from the ground to the ^1L_b state is usually weak and the transition dipole moment parallel to the long-axis, it is a strong short-axis transition for the ^1L_a excitation. Weber[13]

Received: December 14, 2016
Revised: January 31, 2017
Published: January 31, 2017

DOI: 10.1021/acs.jpca.6b12605
J. Phys. Chem. A 2017, 121, 1597−1606

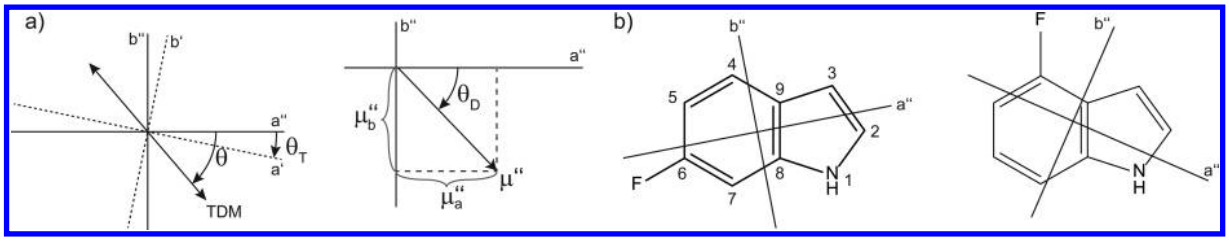

Figure 1. (a) Definition of the negative signs of the angles θ, θ_T, and θ_D. The angle θ defines the orientation of the TDM vector, θ_T the rotation of the principal axis frame upon electronic excitation, and θ_D the orientation of the dipole moment vector. (b) Structures of 6-fluoroindole and 4-fluoroindole in their respective principle axis frames with the atomic numbering of the heavy atoms of the indole chromophore.

adapted this nomenclature to describe the lowest singlet states in indole, where the transition dipole moment vectors for the ^1L_a and ^1L_b states are almost perpendicular and the ^1L_a state has a considerably higher dipole moment than the ^1L_b state.[14,15] However, due to the reduced symmetry of indole the transition moments are only close to the symmetry axis and strictly speaking, both run through bonds. Thus, already for bare indole, there will be some amount of mixing of the two states. Upon introduction of off-axis substituents, the situation gets worse and a clear distinction between the a and the b labels will become increasingly difficult.

Although modifications at position 5 of the indole chromophore (cf. Figure 1) influence the energetic positions of the two excited states, they mostly retain the respective electronic nature: The transition to the ^1L_a is dominated by a LUMO ← HOMO excitation while the ^1L_b state is a nearly equal mixture of (LUMO+1)← HOMO and LUMO ← (HOMO−1) contributions.[16] In a previous study, we observed that approximate coupled-cluster calculations (CC2) predict a loss of the ^1L_a and ^1L_b electronic identities of 6-methoxyindole due to heavy mixing of both electronically excited states.[17] Interestingly, this leads to a disagreement between theory and experiment regarding the absolute orientation of the transition dipole moment (TDM), a parameter which is often used to identify the nature of the excited state in the gas phase. This is even more surprising, as for 5-methoxyindole this effect does not occur.[16] It raises the question whether the excited state mixing is dependent on the position and/or the nature of the substituent and whether the predicted couplings can be quantified experimentally. Furthermore, we have to test whether the orientation of the transition dipole moment remains an unambiguous characteristic for the nature of the excited state of substituted indoles.

Here, we investigate the systems 4- (4FI) and 6-fluoroindole (6FI) with rotationally resolved electronic Stark spectroscopy and compare the results to high-level *ab initio* calculations. We find that the TDM orientation is not a reasonable identifier of the nature of the excited states for substituted indoles in general. Instead, the experimentally observed changes in the permanent dipole moment upon electronic excitation are in good agreement with the ratio of $^1L_a/^1L_b$ contributions and can be used to assign the nature of the electronically excited state.

TECHNIQUES

Experimental Procedures. 4-Fluoroindole (≥98%) was purchased from Carbolution and 6-fluoroindole (≥98%) from Activate Scientific. All samples were used without further purification. To record rotationally resolved electronic spectra of 4-fluoroindole (6-fluoroindole), the samples were heated to 120 °C (144 °C) and coexpanded with 150 mbar (550 mbar) of argon into the vacuum through a 200 μm nozzle. After the expansion a molecular beam was formed using two skimmers (1 mm and 3 mm) linearly aligned inside a differentially pumped vacuum system consisting of three vacuum chambers. The molecular beam was crossed at right angles with the laser beam 360 mm downstream of the nozzle. To create the excitation beam, 7.5 W of the 514 nm line of an Ar^+-ion (Coherent, Sabre 15 DBW) pumped a single frequency ring dye laser (Sirah Matisse DS) operated with Rhodamine 6G. The fluorescence light of the dye laser was frequency doubled in an external folded ring cavity (Spectra Physics Wavetrain) with a resulting power of about 12 mW during the experiments. The fluorescence light of the samples was collected perpendicular to the plane defined by laser and molecular beam by an imaging optics setup consisting of a concave mirror and two plano-convex lenses onto the photocathode of a UV enhanced photomultiplier tube (Thorn EMI 9863QB). A detailed description of the experimental setup for the rotationally resolved laser-induced fluorescence spectroscopy has been given previously.[18,19] To record rotationally resolved electronic Stark spectra, a parallel pair of electro-formed nickel wire grids (18 mesh per mm, 50 mm diameter) with a transmission of 95% in the UV was placed inside the detection volume, one above and one below the molecular beam−laser beam crossing with an effective distance of 23.49 ± 0.05 mm.[20] In this setup the electric field is parallel to the polarization of the laser radiation. With an achromatic $\lambda/2$ plate (Bernhard Halle, 240−380 nm), mounted on a linear motion vacuum feedthrough, the polarization of the incoming laser beam can be rotated by 90° inside the vacuum.

Computational Methods. *Quantum Chemical Calculations.* Structure optimizations were performed using the second-order approximate coupled cluster singles and doubles model (CC2) with the resolution-of-the-identity approximation (RI)[21−23] and Dunning's correlation consistent basis sets of valence triple-ζ quality (cc-pVTZ).[24,25] The equilibrium geometries of the electronic ground and the lowest excited singlet states were additionally calculated by taking spin-component scaling (SCS) modifications into account.[26] With the NumForce script[27] vibrational frequencies and zero-point corrections to the adiabatic excitation energies were obtained. In all cases, the TURBOMOLE program suite was employed.[28]

To obtain the excited singlet state energies, wave functions, transition dipole moments and static dipole moments, we additionally performed combined density functional theory/multireference configuration interaction (DFT/MRCI)[29] calculations in a one-particle basis of closed-shell Kohn−Sham BH-LYP[30] orbitals at the optimized SCS-CC2 geometries. In the semiempirical DFT/MRCI approach, dynamic electron correlation is taken care of by employing Kohn−Sham orbital energies and scaled two-electron integrals in the diagonal Hamiltonian matrix elements whereas static correlation is

DOI: 10.1021/acs.jpca.6b12605
J. Phys. Chem. A 2017, 121, 1597−1606

Table 1. Summary of the Rotational Constants of 4-, 5-, and 6-Fluoroindole in the Lowest Three Singlet States together with the Changes upon Excitation, the Respective Inertial Defects ΔI, and the Axis Reorientation Angles θ_T (cf. Figure 1), Calculated at CC2- and SCS-CC2/cc-pVTZ Levels of Theory

	4-Fluoroindole									
	CC2					SCS-CC2				
	S_0	S_1	S_2	ΔS_1	ΔS_2	S_0	S_1	S_2	ΔS_1	ΔS_2
A/MHz	2203.4	2154.6	–	−48.8	–	2200.4	2142.0	2182.0	−58.5	−18.4
B/MHz	1470.1	1441.7	–	−28.3	–	1465.9	1438.2	1422.7	−27.7	−43.3
C/MHz	881.8	863.8	–	−18.0	–	879.8	860.5	861.2	−19.3	−18.6
ΔI/amu Å^2	0.00	0.00	–	0.00	–	0.00	0.00	0.00	0.00	0.00
θ_T/deg	–	+1.3	–	–	–	–	+0.6	−1.4	–	–
	5-Fluoroindole									
	CC2[38]					SCS-CC2				
	S_0	S_1	S_2	ΔS_1	ΔS_2	S_0	S_1	S_2	ΔS_1	ΔS_2
A/MHz	3520	3395	–	−125	–	3518	3376	–	−142	–
B/MHz	1019	1018	–	−1	–	1017	1016	–	−1	–
C/MHz	790	783	–	−7	–	789	781	–	−8	–
ΔI/amu Å^2	0.00	0.00	–	0.00	–	0.00	0.00	–	0.00	–
θ_T/deg	–	±0.6	–	–	–	–	+0.5	–	–	–
	6-Fluoroindole									
	CC2					SCS-CC2				
	S_0	S_1	S_2	ΔS_1	ΔS_2	S_0	S_1	S_2	ΔS_1	ΔS_2
A/MHz	3478.8	3335.5	–	−143.3	–	3474.4	3328.2	3423.1	−146.2	−51.3
B/MHz	1027.5	1031.7	–	4.2	–	1024.8	1021.5	1007.4	−3.3	−17.4
C/MHz	793.2	788.0	–	−5.2	–	791.4	781.6	778.3	−9.8	−13.1
ΔI/amu Å^2	0.00	0.00	–	0.00	–	0.00	0.00	0.00	0.00	0.00
θ_T/deg	–	−0.6	–	–	–	–	±0.0	±0.0	–	–

addressed through a truncated MRCI expansion. To avoid double counting of dynamic correlation, configurations with energies exceeding the highest reference state energy by at least 1.0 E_h are discarded, and all off-diagonal elements are scaled by an energy dependent damping function. In the DFT/MRCI calculations, eigenvectors and eigenvalues of the 10 lowest-lying singlet states were determined. The initial MRCI reference space comprised all single and double excitations from the four highest occupied MOs to the four lowest unoccupied MOs of the ground state Kohn−Sham determinant. All configurations contributing to one of the 10 lowest-lying eigenvectors of the initial DFT/MRCI calculation with a squared coefficient of at least 0.003 were used to span the reference space of the final DFT/MRCI run.

Fits of the Rovibronic Spectra using Evolutionary Algorithms. Evolutionary algorithms allow us to make a quick and successful automatic assignment of the rotationally resolved spectra, even for large molecules and dense spectra.[31−34] Besides a correct Hamiltonian to describe the spectrum and reliable intensities inside the spectrum, an appropriate search method is needed. Evolutionary strategies are a powerful tool to handle complex multiparameter optimizations and find the global optimum. For the analysis of the presented high-resolution spectra we used the covariance matrix adaptation evolution strategy (CMA-ES), which is described in detail elsewhere.[35,36] For the analysis of rotationally resolved electronic Stark spectra a new Stark Hamiltonian is needed with its matrix elements given in ref 20. The intensities of the rotational lines are calculated from the eigenvectors of the Stark Hamiltonian and the direction cosine matrix elements. The static electric field mixes the rovibronic eigenstates, so that J, K_a, and K_c are no good (pseudo-) quantum numbers anymore, M is the only remaining good quantum number.

RESULTS

Computational Results. Table 1 collects the structural properties of 4FI and 6FI, calculated at CC2- and SCS-CC2/cc-pVTZ level of theory. These are the rotational constants in the electronic ground and lowest two excited states, their changes upon excitation, the inertial defects[52] in the respective states and the axis reorientation angles.

The axis reorientation angle describes the rearrangement of the inertial axis system after electronic excitation. For planar molecules it is described by a single angle θ_T which rotates the axes a'' and b'' in the electronic ground state about the c-axis onto the respective axes in the excited state (cf. Figure 1). The absolute orientation of θ_T can be inferred from *ab initio* geometries of both states according to ref.[37]

$$\tan(\theta_T) = \frac{\sum_i m_i(a_i' b_i'' - b_i' a_i'')}{\sum_i m_i(a_i' a_i'' + b_i' b_i'')} \quad (1)$$

The doubly primed coordinates refer to the coordinates of the ith atom in the principal axis system (PAS) of the electronic ground state, the single primed to those in the excited state, while m_i is the atomic mass of the ith atom in the molecule. This yields an absolute angle of $\theta_T = +1.3°$ for 4FI and $\theta_T = -0.6°$ for 6FI based on the genuine CC2 calculations (cf. Table 1).

From the calculated inertial defects, which are a measure for the nonplanarity of a molecule, we deduce a planar equilibrium structure of both molecules in all states.

Table 2 summarizes all further molecular parameters and compares them to those of 5-fluoroindole (5FI).[38] Among

DOI: 10.1021/acs.jpca.6b12605
J. Phys. Chem. A 2017, 121, 1597−1606

Table 2. Summary of the Theoretical Results at CC2/cc-pVTZ, SCS-CC2/cc-pVTZ, and DFT/MRCI Levels of Theory[a]

	CC2/cc-pVTZ								
	4-fluoroindole			5-fluoroindole			6-fluoroindole		
state	S_0	S_1	S_2	S_0	S_1	S_2	S_0	S_1	S_2
LUMO ← HOMO	–	0.47	–	–	−0.26[38]	–	–	0.87	–
LUMO+1 ← HOMO	–	0.46	–	–	−0.30[38]	–	–	−0.33	–
LUMO ← HOMO−1	–	−0.71	–	–	0.87[38]	–	–	0.22	–
f	–	0.04	–	–	0.07	–	–	0.09	–
μ/D	3.42	2.92	–	3.70[40]	3.31[40]	–	2.88	5.17	–
μ_a/D	2.82	2.57	–	3.27[40]	3.14[40]	–	2.53	4.60	–
μ_b/D	1.94	1.37	–	1.73[40]	1.05[40]	–	1.39	2.35	–
θ_D/deg	−35	−28	–	−28[40]	−19[40]	–	−29	−27	–
θ/deg	–	−54	–	–	+67	–	–	−44	–
ν_0/cm^{-1}	–	36814	–	–	35144[38]	–	–	35924	–
	SCS-CC2/cc-pVTZ								
	4-fluoroindole			5-fluoroindole			6-fluoroindole		
state	S_0	S_1	S_2	S_0	S_1	S_2	S_0	S_1	S_2
LUMO ← HOMO	–	0.31	0.90	–	0.12	–	–	0.60	0.76
LUMO+1 ← HOMO	–	0.54	−0.24	–	0.38	–	–	−0.44	0.19
LUMO ← HOMO−1	–	−0.74	–	–	0.88	–	–	0.56	−0.52
f	–	0.02	0.13	–	0.06	–	–	0.05	0.08
μ/D	3.42	2.98	5.58	3.70	3.29	–	2.88	3.40	5.57
μ_a/D	2.79	2.58	5.50	3.28	3.09	–	2.55	3.03	5.24
μ_b/D	1.98	1.49	0.94	1.71	1.12	–	1.33	1.55	1.90
θ_D/deg	−35	−30	−10	−28	−20	–	−27	−27	−20
θ/deg	–	−65	−14	–	+59	–	–	−17	−83
ν_0/cm^{-1}	–	36432	39841	–	34506	–	–	35745	39177
	DFT/MRCI[b]								
	4-fluoroindole			5-fluoroindole			6-fluoroindole		
state	S_0	S_1	S_2	S_0	S_1	S_2	S_0	S_1	S_2
LUMO ← HOMO	–	0.38	−0.90	–	−0.38	–	–	−0.56	−0.67
LUMO+1 ← HOMO	–	0.51	0.20	–	−0.31	–	–	0.44	−0.30
LUMO ← HOMO−1	–	−0.66	−0.11	–	0.76	–	–	−0.56	0.56
f	–	0.03	0.20	–	0.08	–	–	0.06	0.10
μ/D	3.51	2.84	5.84	3.83	3.24	–	3.00	3.76	5.00
μ_a/D	2.81	2.37	5.78	3.44	3.07	–	2.75	3.47	4.80
μ_b/D	2.11	1.57	0.86	1.68	1.03	–	1.20	1.47	1.40
θ_D/deg	−37	−34	−8	−26	−19	–	−24	−23	−16
θ/deg	–	−68	−12	–	+63	–	–	−21	−84
ν_0/cm^{-1}	–	36919	39658	–	35669	–	–	36424	38865

[a]This includes the coefficients of the most dominant transitions according to the $S_1 \leftarrow S_0$ and $S_2 \leftarrow S_0$ excitation of 4-, 5- and 6-fluoroindole. The labeling of the orbitals involved was adapted to those of indole according to their contours, cf text. Besides, the respective oscillator strengths f, the absolute dipole moments μ, their individual components along the main inertial axes μ_a and μ_b (μ_c is zero due to the planarity of the molecules) and their angle θ_D with the main inertial a-axis (cf. Figure 1) as well as the adiabatic excitation energies ν_0 are listed. [b]DFT/MRCI calculations are based on the optimized SCS-CC2/cc-pVTZ geometries in the respective states.

other, this includes the magnitude of the ground and excited state dipole moments μ and the angle θ of the TDM vector with the main inertial a-axis, calculated at the respective equilibrium geometry. According to Figure 1, a negative θ angle belongs to a clockwise rotation of the TDM vector from the a-axis. While for 4FI and 5FI the magnitude of the permanent dipole moment decreases upon excitation to the lowest electronically excited state by around 15% relative to the dipole moment in the S_0 state, the opposite behavior is observed for 6FI. However, there are deviations in the magnitude of the predicted dipole moment for 6FI. Genuine CC2 predicts a considerably larger increase of more than 2 D compared to 0.5−0.8 D at SCS-CC2 and DFT/MRCI level of theory.

Regarding the TDM orientation, the angle θ is calculated to be negative for 4FI and 6FI in both states at the respective equilibrium geometries. This means that the TDM vector is rotated clockwise from the a-axis. Although the S_1 and S_2 state vectors of both molecules make an angle of around 60°, their orientations within the PAS differ significantly. While for 4FI the S_2 state vector is calculated to be close to the a-axis, this is the case for the S_1 state vector of 6FI.

The nature of an excited state can be quantified based on the coefficients of the molecular orbital excitations which are compiled in Table 2 for 4FI and 6FI in comparison to the respective values of 5FI.[38] As stated in the introduction, the ^1L_a is dominated by a LUMO ← HOMO excitation, while the ^1L_b is an equal mixture of LUMO ← (HOMO−1) and (LUMO+1) ← HOMO contributions. Depending on the size of the basis

DOI: 10.1021/acs.jpca.6b12605
J. Phys. Chem. A 2017, 121, 1597−1606

set Rydberg-type orbitals may lie between π-orbitals for substituted indoles.[38,39] This is also the case for the systems investigated, shifting the (LUMO+1) to higher orbitals and, thus, modifying the excitation scheme slightly. In order to make a better comparison, the labeling of the orbitals involved was adapted to those of indole according to their contours. For 4FI and 5FI, all methods agree well with the excitation scheme mentioned before and predict that the leading contributions to the S_1 can be assigned to the ^1L_b. Furthermore, for 4FI the S_2 is dominated by the LUMO ← HOMO transition which also falls within the scheme. For 6FI, however, this is not the case. While genuine CC2 predicts the ^1L_a-contribution to be the leading term for the S_1, SCS-CC2 and DFT/MRCI show strong mixing of ^1L_a and ^1L_b contributions in both electronically excited states. In the S_1 state the ^1L_b contributions have a slightly stronger influence, but this amounts only to 15−20% whereas it is 50−90% for 4FI and 5FI. For the S_2 we observe a comparable situation with leading contributions from the ^1L_a. This is reflected by the oscillator strength of the transitions which is higher for the ^1L_a compared to the ^1L_b. For 6FI they are nearly equal, while for 4FI the oscillator strength of the S_1 is much smaller than the one of the S_2 which is to be expected of ^1L_a and ^1L_b-transitions.

Rotationally Resolved Fluorescence Spectra. The rotationally resolved spectrum of the electronic origin of 4FI is shown in Figure 2, the respective spectrum of 6FI is shown in the supporting online material. The spectra were analyzed with a rigid-rotor Hamiltonian including axis reorientation and are accompanied by a simulation based on the best molecular parameter as obtained from the fitting routine. The obtained molecular constants are compiled in Table 3. For both molecules, we observe an excellent agreement between the experimental and theoretical (cf. Table 1) values of the rotational constants with a mean deviation of 0.2%, even though the calculated rotational constants are equilibrium values while the experimental rotational constants are zero-point vibrationally averaged. For 5-cyanoindole the analysis of vibrational averaging on the rotational constants showed that the equilibrium parameters have a better agreement with the experiment than the vibrationally averaged parameters.[41] The population of the rotational states can be described by a two temperature model, proposed by Wu and Levy[42] with $n_i = e^{-E_i/kT_1} + \omega e^{-E_i/kT_2}$ and n_i as the population of the ith rovibronic level at energy E_i, k as the Boltzmann constant, T_1 and T_2 as the two temperatures, and ω as a weighting factor, which is modeling the contribution from T_2. The best fitting results for both temperatures and the weighting factor are given in Table 3. The band type of each spectrum is an ab-hybrid with 20% a-type and 80% b-type for 4FI and 84% a-type and 16% b-type for 6FI. In the case of 4FI, this leads to an in-plane angle of the TDM vector with the inertial a-axis of $\theta = \pm 63.1°$ and $\theta = \pm 23.5°$ for 6FI. While the adiabatic excitation energies are in good agreement with previously published results,[43,44] we observe a slight deviation of the excited state lifetime for 6FI compared to the value reported by Sulkes and Borthwick.[43]

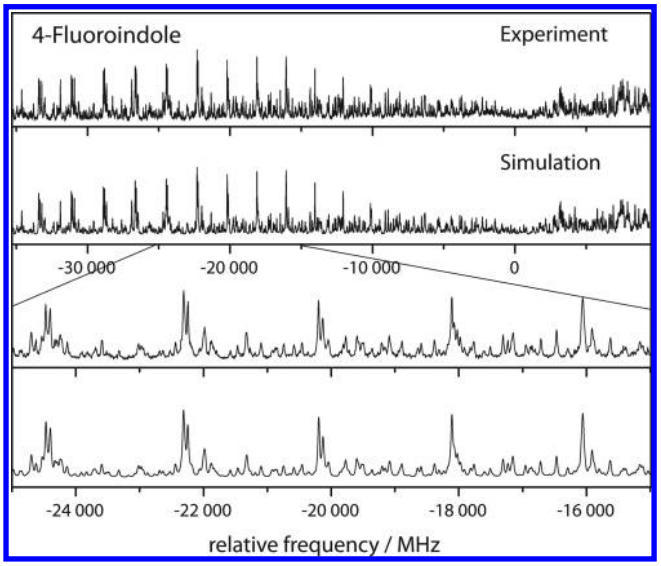

Figure 2. Rotationally resolved spectrum of the electronic origin of 4-fluoroindole, along with a simulation using the best CMA-ES fit parameters, given in Table 3.

Orientation of the Transition Dipole Moment. While the magnitude of θ can be determined from the experimentally observed band-type, no information about its sign is contained. Only the projection of the TDM onto the a-axis can be inferred from the band type. However, this ambiguity can be lifted by the determination of the axis reorientation angle θ_T and also by the investigation of isotopologues. Both methods are made use of here.

Axis reorientation leads to a change of intensities of the rovibronic lines. From the fit of the intensity pattern we can determine the *relative* sign between θ_T and θ. That means, that a +/+ combination and a −/− combination lead to the same intensity pattern, which is different from the pair +/− or −/+. For 4FI and 6FI, the intensity analysis yields the same sign for the two angles (cf. Table 3). Since the absolute orientation of θ_T can be determined from the *ab initio* calculations to be positive for 4FI and negative for 6FI (cf. Table 1), the absolute sign of θ is determined to be positive for 4FI and negative for 6FI.

Another method to determine the absolute angle of θ is to analyze the spectra of the same molecule where one atom is replaced by an isotope. An off-axis exchange of one hydrogen atom by deuterium leads to a rotation of the PAS toward the heavier deuterium but has no influence on the TDM orientation.[45,46] However, the position of the deuteration must be determined first. This was done by comparing the computed rotational constants for all possible singly deuterated isotopomers from the *ab initio* structures with the experimental values, summarized in the supporting online material. The best agreement is obtained for the isotopomer deuterated at position N_1. Consequently, the PAS is rotated clockwise. The molecular constants of [d-N_1]-6FI are also compiled in Table 3, the respective rotationally resolved electronic spectrum is shown in the supporting online material. The decrease in θ by 1° upon deuteration ascertains the result from the analysis of the axis reorientation angle and points to a negative sign for θ in the case of 6FI.

Excited State Dipole Moments. The electronic Stark spectrum of 6FI is shown in Figure 3 and the one for 4FI can be found in the supporting online material. For both molecules the spectra were recorded at a field strength of 397.19 V/cm with the laser light polarized parallel and/or perpendicular to the static electric field. For 6FI, spectra with different field configurations were fitted simultaneously to improve the precision in the determination of the dipole moment.[20] The field configurations are defined by the orientation of the electric field with respect to the polarization

DOI: 10.1021/acs.jpca.6b12605
J. Phys. Chem. A 2017, 121, 1597−1606

Table 3. Molecular Parameters for 4-, 5-, and 6-Fluoroindole in their Ground and First Electronically Excited States from a CMA-ES Fit of the Rovibronic Spectra[a]

	4-fluoroindole	5-fluoroindole[38,40]	6-fluoroindole	[d-N_1] 6-fluoroindole
A''/MHz	2206.51(3)	3519.57(4)	3478.85(6)	3360.77(8)
B''/MHz	1467.26(3)	1019.79(1)	1029.04(1)	1021.92(2)
C''/MHz	881.39(2)	790.87(1)	794.27(1)	783.79(2)
$\Delta I''$/amu Å^2	−0.09	−0.15	−0.11	−0.13
μ_a''/D	2.62(3)	3.27(1)	2.47(2)	–
μ_b''/D	2.19(2)	1.56(1)	0.44(8)	–
μ_c''/D	0.00	0.00	0.00	–
μ''/D	3.41(4)	3.62(1)	2.51(3)	–
θ_D''/deg	±40(1)	±26(1)	±10(4)	–
A'/MHz	2154.22(3)	3386.34(3)	3336.12(7)	3226.93(8)
B'/MHz	1442.88(3)	1019.83(1)	1030.40(2)	1023.07(2)
C'/MHz	864.40(3)	784.09(1)	787.57(2)	777.11(2)
$\Delta I'$/amu Å^2	−0.20	−0.25	−0.26	−0.27
ΔA/MHz	−52.29(1)	−133.23(2)	−142.73(1)	−133.84(1)
ΔB/MHz	−24.38(1)	+0.043(1)	1.36(1)	1.15(1)
ΔC/MHz	−16.99(1)	−6.78(1)	−6.70(1)	−6.68(1)
μ_a'/D	2.39(3)	3.14(1)	3.31(2)	–
μ_b'/D	1.80(2)	1.07(2)	0.69(6)	–
μ_c'/D	0.00	0.00	0.00	–
μ'/D	2.99(4)	3.32(2)	3.38(3)	–
θ_D'/deg	±37(1)	±19(1)	±12(3)	–
T_1/K	6.61(1)	2.5	7.07(1)	7.63(1)
T_2/K	6.91(3)	4.8	5.92(1)	6.33(1)
ω	0.11(1)	0.2	0.08(1)	0.99(1)
θ/deg	±63.1(1)	±59(1)	±23.5(1)	±22.5(1)
θ_T/deg	±0.72(7)	±0.8(1)	±0.13(5)	–
ν_0/cm^{-1}	35 641.37(1)	34 335.89(1)	34 977.54(1)	34 987.97(1)
τ/ns	6.0(1)	12(4)	6.4(1)	8.5(2)

[a]Changes of the rotational constants are defined as $\Delta B_g = B_g' - B_g''$, with B_g as rotational constants with respect to the inertial axes $g = a, b, c$. Double-primed constants belong to the ground state and single-primed to the excited state. The center frequency of the respective band is ν_0 and τ is the lifetime of the lowest electronically excited state. Additionally, the unsigned Cartesian coordinates μ_i with $i = a, b, c$, the values of the absolute dipole moments μ in the ground and lowest electronically excited state and the angles of the respective dipole moments with the main inertial a-axis θ_D are given. The uncertainties of the parameters are given in parentheses and are obtained as standard deviations by performing a quantum number assigned fit.

of the exciting laser radiation. If the electric field is 100% parallel (perpendicular) to the polarization of the exciting laser radiation, only transition with $\Delta M = 0$ ($\Delta M = \pm 1$) are allowed. Because of technical reasons we always observe a mixture of 80% $\Delta M = 0$ and 20% $\Delta M = \pm 1$ transitions without the half-wave plate and 20% $\Delta M = 0$ and 80% $\Delta M = \pm 1$ with the half-wave plate inside the laser beam. During the analysis of the spectra the rotational constants, the rotational temperatures, and the relative band origin were kept constant at the values from the fit of the field free spectrum. In Table 3 the experimentally observed dipole moments and their components along the inertial axes are listed. Here, the overall dipole moments are calculated from the respective components along each axis μ_i ($i = a, b, c$) with μ_c being zero for both states. For 4FI a total dipole moment of 3.41 D in the ground and 2.99 D in the lowest electronically excited state is observed. In contrast to that, the dipole moment increases from 2.51 to 3.38 D upon electronic excitation for 6FI.

Fluorescence Quantum Yields. The pure radiative (natural) lifetime of a transition from state i to state f is given by

$$\tau_{nat} = \frac{c^3}{8\pi h \nu_{fi}^3} \frac{6\epsilon_0 \hbar^2}{\mu_{fi}^2} \tag{2}$$

where ν_{fi} is the transition frequency and μ_{fi} the transition dipole moment. The latter can be calculated from the dimensionless oscillator strength f:

$$\mu_{fi} = \sqrt{\frac{fhe^2}{8\pi m_e \nu_{fi}}} \tag{3}$$

The ratio of the experimental lifetime τ_{exp}, which is the inverse of the sum of all radiative and the nonradiative deactivation paths and the natural lifetime τ_{nat}, as the inverse of the fluorescence rate constant k_f yields the fluorescence quantum yield:

$$Q = \frac{k_f}{k_f + \sum k_{nr}} = \frac{k_f}{\sum k_i} = \frac{\tau_{\exp}}{\tau_{nat}} \tag{4}$$

Using the oscillator strengths f and the transition frequencies ν_{fi} from the *ab initio* calculations (cf. Table 2) and the experimentally determined life times from Table 3, the fluorescence quantum yields for 4FI, 5FI, and 6FI can be calculated to be 0.2, 0.8, and 0.6, respectively.

DISCUSSION

To determine the nature of the electronically excited state of indole derivatives commonly the orientation of the transition

DOI: 10.1021/acs.jpca.6b12605
J. Phys. Chem. A 2017, 121, 1597−1606

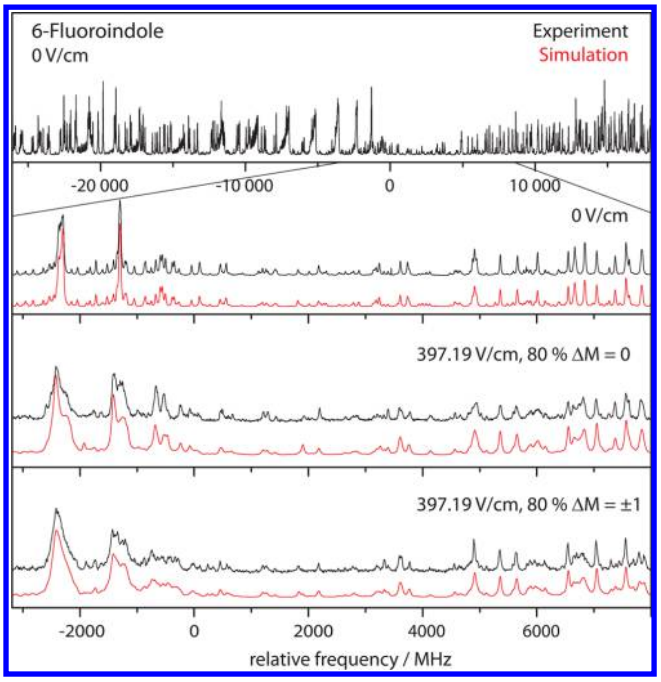

Figure 3. Rovibronic spectrum of the electronic origin of 6-fluoroindole at 0 V/cm with a zoomed part of the spectrum at 0 and 397.19 V/cm with both field configurations along with a simulation using the best CMA-ES fit parameters, given in Table 3.

dipole moment is used.[14,15,47,48] For the ^1L_b the vector is rotated counterclockwise from the *a*-axis by a positive angle θ, whereas the relative sign of θ is negative for the ^1L_a, according to a clockwise rotation (cf. Figure 4). Since the position and orientation of the PAS change due to the addition of the fluorine atom at different positions, all fluoro-substituted indole derivatives have to be rotated into a common reference frame to evaluate the electronic nature of the excited states. The most obvious choice is the pseudo C_2-axis going through C2 and the middle of the C5−C6 bond. This leads to a new angle θ_{ref} (cf. Figure 4), which is compiled for all investigated systems in Table 4.

We start with the discussion of the theoretical results. For 5FI, the angle θ_{ref} for the S_1 state is in good agreement with the one for an ^1L_b state in indole and can be unambiguously assigned as an ^1L_b state based on the TDM orientation, which gets also confirmed by the experimental results.[38] Unfortunately, all efforts to optimize the second electronically excited state failed, because optimization runs into a geometry, where S_1 and S_2 cross and L_a and L_b change their order. Distortion of the 5FI geometry along coordinates which are known from previous studies[14,15,49] to favor the L_a geometry failed. Thus, we assume the S_2 state minimum to be close to a conical intersection between the L_a and L_b, like it is the case for indole.[14] Surprisingly, theory predicts the angle θ_{ref} to be negative for 4FI and 6FI in both excited states. While the $S_0 \rightarrow S_2$ TDM orientation of 4FI resembles the one of the ^1L_a state in indole, it is not possible to determine the nature of the other excited states from their TDM orientation. For 4FI the $S_0 \rightarrow S_1$ and for 6FI the $S_0 \rightarrow S_2$ TDM vector lies almost along the inertial *b*-axis of indole, while the $S_0 \rightarrow S_1$ vector of 6FI is close to the *a*-axis. This points toward a mixing of ^1L_a and ^1L_b character in the respective states, which can be inferred from the coefficients of the orbital excitations (cf. Table 2). Interestingly, the adiabatic energy gap between S_1 and S_2 is nearly identical in 4FI and 6FI. While genuine CC2 (SCS-CC2) calculations only predict an amount of 7(1) % LUMO ← HOMO excitation for 5FI in the S_1 state, it increases to 22(11) % for 4FI and to 75(36) % for 6FI. Thus, the negative sign of θ can be explained with the increased amount of ^1L_a character, as already proposed for 4- and 6-methoxyindole by Albinsson and Norden.[47]

This assignment is confirmed experimentally for 6FI, but stands in contrast to the experimentally determined positive sign of θ for 4FI, as it was also the case for 6-methoxyindole.[17] This shows that a deviating TDM orientation between experiment and theory cannot be traced back to a specific substituent or its position at the chromophore. Instead, the individual molecule and its photophysical properties seem to be responsible for this ambiguity. In this context, one has to keep in mind that the calculated TDM orientation is determined for a vertical absorption at a given geometry, while the experimental value is derived from the fluorescence of the 0−0 transition. Hence, for systems where the TDM vector tends to change its orientation quite easily, slightest geometry changes upon excitation can lead to completely different θ angles. In conclusion, we state that the absolute orientation of the transition dipole moment is not a useful identifier of the electronic nature for substituted indoles in general.

Thus, other characteristics are needed to identify the nature of the excited states. One of these is the permanent electric dipole moment of the excited states. While the magnitude of the dipole moment of the ^1L_b is slightly smaller than the one of the ground state,[50] it increases considerably upon excitation to the ^1L_a state.[14,51] Comparing the experimental and calculated dipole moments from Table 2 and 3 shows that the changes in

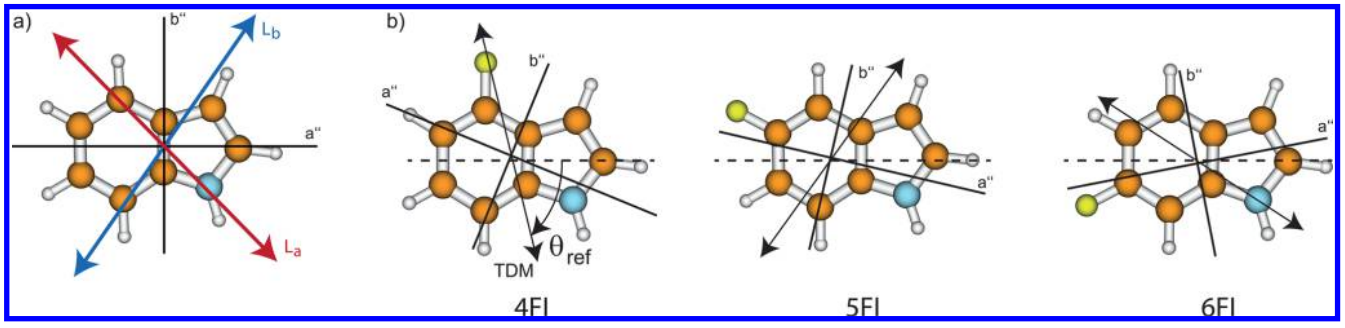

Figure 4. (a) TDM vector orientations for the S_1 (blue) and S_2 (red) states of indole at the CC2/cc-pVTZ level of theory.[14] (b) Definition of θ_{ref} which describes the angle of the TDM vector with the pseudo C_2 axis of indole and overview of the $S_0 \rightarrow S_1$ TDM vectors, calculated at CC2/cc-pVTZ level of theory.

DOI: 10.1021/acs.jpca.6b12605
J. Phys. Chem. A 2017, 121, 1597−1606

Table 4. Summary of the Angles θ_{ref} of the S_1 and S_2 State TDM Vectors with the Pseudo C_2 Axis of Indole (cf. Figure 4) for 4-, 5- and 6-Fluoroindole at Various Levels of Theory

	indole[14]		4FI			5FI			6FI		
	CC2	DFT/MRCI	CC2	SCS-CC2	DFT/MRCI	CC2	SCS-CC2	DFT/MRCI	CC2	SCS-CC2	DFT/MRCI
θ_{ref} S_1/deg	+55	+40	−78	−89	−92	+55	+47	+51	−32	−5	−9
θ_{ref} S_2/deg	−46	−37	–	−38	−36	–	–	–	–	−71	−72

the magnitude are well reproduced by the *ab initio* calculations with the exception of the S_1 dipole moment of 6FI derived from genuine CC2 calculations. Here, the question arises, if the CC2 optimized state is indeed the S_1 state. The magnitude of the permanent dipole moment, and the oscillator strength are rather in line with an assignment as S_2 state. By and large, the properties determined from DFT/MRCI wave functions resemble the SCS-CC2 values. The strong mixing of the lowest excited singlet states makes the coefficients of the LUMO ← HOMO and of the LUMO+1 ← HOMO insufficient parameters for an assignment.

For 4FI, the dipole moment decreases by 0.42 D upon excitation, while for 6FI an increase of 0.87 D is observed. Additionally, we compare the results to those of 5FI for which the nature of the lowest excited singlet state was ascertained to be ^1L_b.[38] For 5FI, a small decrease in the permanent dipole moment of 0.3 D upon excitation to the S_1 state has been reported.[40]

Consequently, a small perturbation of the lowest electronically excited state due to an increased amount of LUMO ← HOMO character, as it is observed for 4FI, only affects the TDM orientation, whereas the change in the permanent dipole moment upon excitation and thus, the electronic nature of the excited state remains ^1L_b-like. For 6FI, theory predicts a heavily mixed character of both electronically excited states. Although the experiment shows that the permanent dipole moment increases upon excitation, the increase is much smaller than for a pure ^1L_a state like in indole.[14,51] Thus, an assignment to a pure ^1L_a or ^1L_b state is not possible. This reflects the mixed nature of the excited state as predicted by the *ab initio* calculations.

CONCLUSIONS

The structures of 4- and 6-fluoroindole in the ground and lowest electronically excited state and their dipole moments in both states have been determined by means of rotationally resolved electronic Stark spectroscopy in combination with high level *ab initio* calculations. With the exception of the TDM orientation the experimental and theoretical results reveal mainly ^1L_b character for the S_1 and ^1L_a character for the S_2 state of 4FI, while both excited states of 6FI are strongly mixed and not unambiguously assignable. This can be inferred from the change of the permanent electric dipole moments upon excitation and coefficients of the orbital excitations.

ASSOCIATED CONTENT

Supporting Information

The Supporting Information is available free of charge on the ACS Publications website at DOI: 10.1021/acs.jpca.6b12605.

Comparison of the experimentally determined rotational constants, rotationally resolved spectra, and rovibronic spectra (PDF)

AUTHOR INFORMATION

Corresponding Author

*(M.S.) E-mail: mschmitt@uni-duesseldorf.de.

ORCID

Martin Wilke: 0000-0002-9430-1909

Christel M. Marian: 0000-0001-7148-0900

Author Contributions

‖These authors contributed equally

Notes

The authors declare no competing financial interest.

ACKNOWLEDGMENTS

We gratefully acknowledge the help of Leo Meerts for making available the analysis of the electronic Stark spectrum with the CMA-ES algorithm. M.S. thanks the Deutsche Forschungsgemeinschaft (SCHM 1043/12-3) and C.B. the Alexander von Humboldt foundation through a Feodor-Lynen fellowship for financial support of this work. Computational support and infrastructure was provided by the "Center for Information and Media Technology" (ZIM) at the Heinrich-Heine-University Düsseldorf (Germany).

REFERENCES

(1) Lang, K.; Chin, J. W. Cellular Incorporation of Unnatural Amino Acids and Bioorthogonal Labeling of Proteins. *Chem. Rev.* **2014**, *114*, 4764−4806.

(2) Budisa, N.; Rubini, M.; Bae, J. H.; Weyher, E.; Wenger, W.; Golbik, R.; Huber, R.; Moroder, L. Global Replacement of Tryptophan with Aminotryptophans Generates Non-Invasive Protein-Based Optical pH Sensors. *Angew. Chem., Int. Ed.* **2002**, *41*, 4066−4069.

(3) Hyun Bae, J.; Rubini, M.; Jung, G.; Wiegand, G.; Seifert, M. H. J.; Azim, M. K.; Kim, J.-S.; Zumbusch, A.; Holak, T. A.; Moroder, L.; et al. Expansion of the Genetic Code Enables Design of a Novel Gold Class of Green Fluorescent Proteins. *J. Mol. Biol.* **2003**, *328*, 1071−1081.

(4) Wong, C.-Y.; Eftink, M. R. Incorporation of Tryptophan Analogues into Staphylococcal Nuclease, Its V66W Mutant, and Δ137−149 Fragment: Spectroscopic Studies. *Biochemistry* **1998**, *37*, 8938−8946.

(5) Waegele, M. M.; Tucker, M. J.; Gai, F. 5-Cyanotryptophan as an infrared probe of local hydration status of proteins. *Chem. Phys. Lett.* **2009**, *478*, 249−253.

(6) Twine, S. M.; Szabo, A. G. Fluorescent amino acid analogs. *Methods Enzymol.* **2003**, *360*, 104−127.

(7) Hott, J. L.; Borkman, R. F. The non-fluorescence of 4-fluorotryptophan. *Biochem. J.* **1989**, *264*, 297−299.

(8) Martinaud, M.; Kadiri, A. Comparative sensibility of the $S_1 \leftarrow S_0$ and $S_2 \leftarrow S_0$ indole electronic transitions to environment perturbations. The positions of the 0−0 bands in polar media. *Chem. Phys.* **1978**, *28*, 473−485.

(9) Oeltermann, O.; Brand, C.; Engels, B.; Tatchen, J.; Schmitt, M. The structure of 5-cyanoindole in the ground and lowest electronically excited singlet state, deduced from rotationally resolved electronic spectroscopy and ab initio theory. *Phys. Chem. Chem. Phys.* **2012**, *14*, 10266−10270.

(10) Albinsson, B.; Kubista, M.; Nordén, B.; Thulstrup, E. W. Generation and Detection of Intense Cluster Beams. *J. Phys. Chem.* **1989**, *93*, 6646.

(11) Markiewicz, B. N.; Mukherjee, D.; Troxler, T.; Gai, F. Utility of 5-Cyanotryptophan Fluorescence as a Sensitive Probe of Protein Hydration. *J. Phys. Chem. B* **2016**, *120*, 936−944.
(12) Platt, J. R. Classification of Spectra of CataCondensed Hydrocarbons. *J. Chem. Phys.* **1949**, *17*, 484−495.
(13) Weber, G. Fluorescence-polarization spectrum and electronic-energy transfer in tyrosine, tryptophan and related compounds. *Biochem. J.* **1960**, *75*, 335−345.
(14) Brand, C.; Küpper, J.; Pratt, D. W.; Meerts, W. L.; Krügler, D.; Tatchen, J.; Schmitt, M. Vibronic coupling in indole: I. theoretical description of ^1L_a and ^1L_b interactions and the absorption spectrum. *Phys. Chem. Chem. Phys.* **2010**, *12*, 4968−4997.
(15) Küpper, J.; Pratt, D. W.; Meerts, W. L.; Brand, C.; Tatchen, J.; Schmitt, M. Vibronic coupling in indole: II. Investigation of the ^1L_a-^1L_b interaction using rotationally resolved electronic spectroscopy. *Phys. Chem. Chem. Phys.* **2010**, *12*, 4980−4988.
(16) Brand, C.; Oeltermann, O.; Pratt, D. W.; Weinkauf, R.; Meerts, W. L.; van der Zande, W.; Kleinermanns, K.; Schmitt, M. Rotationally resolved electronic spectroscopy of 5-methoxyindole. *J. Chem. Phys.* **2010**, *133*, 024303.
(17) Brand, C.; Oeltermann, O.; Wilke, M.; Schmitt, M. Position Matters: High Resolution Spectroscopy on 6-Methoxyindole. *J. Chem. Phys.* **2013**, *138*, 024321.
(18) Schmitt, M. Spektroskopische Untersuchungen an Wasserstoff-brückenbindungen. Habilitation, Heinrich-Heine-Universität, Math. Nat. Fakultät, Heinrich-Heine-Universität Düsseldorf, 2000.
(19) Schmitt, M.; Küpper, J.; Spangenberg, D.; Westphal, A. Determination of the structures and barriers to hindered internal rotation of the phenol-methanol cluster in the S_0 and S_1 state. *Chem. Phys.* **2000**, *254*, 349−361.
(20) Wilke, J.; Wilke, M.; Meerts, W. L.; Schmitt, M. Determination of ground and excited state dipole moments via electronic Stark spectroscopy: 5-methoxyindole. *J. Chem. Phys.* **2016**, *144*, 044201.
(21) Hättig, C.; Weigend, F. CC2 excitation energy calculations on large molecules using the resolution of the identity approximation. *J. Chem. Phys.* **2000**, *113*, 5154−5161.
(22) Hättig, C.; Köhn, A. Transition moments and excited-state first-order properties in the coupled cluster model CC2 using the resolution-of-the-identity approximation. *J. Chem. Phys.* **2002**, *117*, 6939−6951.
(23) Hättig, C. Geometry optimizations with the coupled-cluster model CC2 using the resolution-of-the-identity approximation. *J. Chem. Phys.* **2003**, *118*, 7751−7761.
(24) Ahlrichs, R.; Bär, M.; Häser, M.; Horn, H.; Kölmel, C. Electronic Structure Calculations on Workstation Computers: The Program System TURBOMOLE. *Chem. Phys. Lett.* **1989**, *162*, 165−169.
(25) Dunning, T. H.; Gaussian, J. basis sets for use in correlated molecular calculations. I. The atoms boron through neon and hydrogen. *J. Chem. Phys.* **1989**, *90*, 1007−1023.
(26) Hellweg, A.; Grün, S.; Hättig, C. Benchmarking the performance of spin-component scaled CC2 in ground and electronically excited states. *Phys. Chem. Chem. Phys.* **2008**, *10*, 4119.
(27) Deglmann, P.; Furche, F.; Ahlrichs, R. An efficient implementation of second analytical derivatives for density functional methods. *Chem. Phys. Lett.* **2002**, *362*, 511−518.
(28) TURBOMOLE V6.5 2013. A development of University of Karlsruhe and Forschungszentrum Karlsruhe GmbH, 1989−2007; TURBOMOLE GmbH: since 2007; available from http://www.turbomole.com., 2013.
(29) Grimme, S.; Waletzke, M. A combination of Kohn-Sham density functional theory and multi-reference configuration interaction method. *J. Chem. Phys.* **1999**, *111*, 5645−5655.
(30) Becke, A. D. A new mixing of Hartree-Fock and local density-functional theories. *J. Chem. Phys.* **1993**, *98*, 1372−1377.
(31) Meerts, W. L.; Schmitt, M.; Groenenboom, G. New applications of the Genetic Algorithm for the interpretation of High Resolution Spectra. *Can. J. Chem.* **2004**, *82*, 804−819.
(32) Meerts, W. L.; Schmitt, M. A new automated assign and analyzing method for high resolution rotational resolved spectra using Genetic Algorithms. *Phys. Scr.* **2006**, *73*, C47−C52.
(33) Meerts, W. L.; Schmitt, M. Application of genetic algorithms in automated assignments of high-resolution spectra. *Int. Rev. Phys. Chem.* **2006**, *25*, 353−406.
(34) Schmitt, M.; Meerts, W. L. In *Handbook of High Resolution Spectroscopy*; Quack, M., Merkt, F., Eds.; John Wiley and Sons: 2011.
(35) Ostermeier, A.; Gawelczyk, A.; Hansen, N.; Davidor, Y.; Schwefel, H.-P.; Männer, R. Step-Size Adaptation Based on Non-Local Use of Selection Information. *Lecture Notes in Computer Science: Parallel Problem Solving from Nature (PPSN III)* **1994**, *866*, 189−198.
(36) Hansen, N.; Ostermeier, A. Completely derandomized self-adaptation in evolution strategies. *Evolutionary Computation* **2001**, *9*, 159−195.
(37) Hougen, J. T.; Watson, J. K. G. Anomalous Rotational Line Intensities in Electronic Transitions of Polyatomic Molecules: Axis-Switching. *Can. J. Phys.* **1965**, *43*, 298−320.
(38) Brand, C.; Oeltermann, O.; Wilke, M.; Tatchen, J.; Schmitt, M. Ground and electronically excited singlet state structures of 5-fluoroindole, deduced from rotationally resolved electronic spectroscopy and *ab initio* theory. *ChemPhysChem* **2012**, *13*, 3134−3138.
(39) Oeltermann, O.; Brand, C.; Wilke, M.; Schmitt, M. Ground and Electronically Excited Singlet State Structures of the syn and anti Rotamers of 5-Hydroxyindole. *J. Phys. Chem. A* **2012**, *116*, 7873−7879.
(40) Wilke, J.; Wilke, M.; Brand, C.; Meerts, W. L.; Schmitt, M. On the Additivity of Molecular Fragment Dipole Moments of 5-Substituted Indole Derivatives. *ChemPhysChem* **2016**, *17*, 2736−2743.
(41) Brand, C.; Happe, B.; Oeltermann, O.; Wilke, M.; Schmitt, M. High resolution spectroscopy of several rovibronically excited bands of 5-cyanoindole - the effect of vibrational averaging. *J. Mol. Struct.* **2013**, *1044*, 21−25.
(42) Wu, Y. R.; Levy, D. H. Determination of the geometry of deuteratedtryptamine by rotationally resolved electronic spectroscopy. *J. Chem. Phys.* **1989**, *91*, 5278−5284.
(43) Sulkes, M.; Borthwick, I. Enhanced photophysical effects in indole due to C-6 chemical group substitutions. *Chem. Phys. Lett.* **1997**, *279*, 315−318.
(44) Barstis, T. L. O.; Grace, L. I.; Dunn, T. M.; Lubman, D. L. Vibronic Analysis of 4-, 5-, and 6-Fluoroindole. *J. Phys. Chem.* **1994**, *98*, 4261−4270.
(45) Schmitt, M.; Krügler, D.; Böhm, M.; Ratzer, C.; Bednarska, V.; Kalkman, I.; Meerts, W. L. A genetic algorithm based determination of the ground and excited ^1L_b state structure and the orientation of the transition dipole moment of benzimidazole. *Phys. Chem. Chem. Phys.* **2006**, *8*, 228−235.
(46) Kang, C.; Yi, J. T.; Pratt, D. W. High resolution electronic spectra of 7-azaindole and its Ar atom van der Waals complex. *J. Chem. Phys.* **2005**, *123*, 094306.
(47) Albinsson, B.; Nordén, B. Excited-State Properties of the Indole Chromophore - Electronic-Transition Moment Directions from Linear Dichroism Measurements - Effect of Methyl and Methoxy Substituents. *J. Phys. Chem.* **1992**, *96*, 6204.
(48) Eftink, M. R.; Selvidge, L. A.; Callis, P. R.; Rehms, A. A. Photophysics of Indole Derivatives: Experimental Resolution of L_a and L_b Transitions and Comparison with Theory. *J. Phys. Chem.* **1990**, *94*, 3469−3479.
(49) Böhm, M.; Tatchen, J.; Krügler, D.; Kleinermanns, K.; Nix, M. G. D.; LeGreve, T. A.; Zwier, T. S.; Schmitt, M. High-resolution and Dispersed Fluorescence Examination of Vibronic bands of Tryptamine: Spectroscopic signatures for L_a/L_b mixing near a conical intersection. *J. Phys. Chem. A* **2009**, *113*, 2456−2466.
(50) Kang, C.; Korter, T. M.; Pratt, D. W. Experimental measurement of the induced dipole moment of an isolated molecule in its ground and electronically excited states: Indole and indole-H_2O. *J. Chem. Phys.* **2005**, *122*, 174301.
(51) Jalviste, E.; Ohta, N. Stark absorption spectroscopy of indole and 3-methylindole. *J. Chem. Phys.* **2004**, *121*, 4730−4739.

DOI: 10.1021/acs.jpca.6b12605
J. Phys. Chem. A 2017, 121, 1597−1606

(52) The inertial defect ΔI is defined as $I_c - I_b - I_a$, where the I_g are the moments of inertia with respect to the main inertial axes $g = a$, b, and c.

DOI: 10.1021/acs.jpca.6b12605
J. Phys. Chem. A 2017, 121, 1597−1606